

TIFR/TH/96-48

August, 1996

hep-ph/yymmdd

## Colour-octet Contributions to $x_F$ Distributions in $J/\psi$ Hado-production at Fixed Target Energies.

Sourendu Gupta and K. Sridhar.

Theory Group, Tata Institute of Fundamental Research,  
Homi Bhabha Road, Bombay 400005, India.

### Abstract

We study  $J/\psi$  production at fixed-target energies, including the colour-octet production mechanisms predicted by NRQCD. In an earlier paper, we found that the octet components were crucial in understanding  $p_T$ -integrated forward ( $x_F > 0$ ) cross-sections. Here we make a detailed comparison of the theoretical predictions with measured  $x_F$  distributions from fixed-target experiments. We find that the model predictions agree well with data. Taking into account higher orders in NRQCD, we argue that  $\sigma(\chi_1)/\sigma(\chi_2) = 0.6$ , in excellent agreement with data. Similiar arguments also predict that  $\sigma(\chi)/\sigma(J/\psi)$  is roughly equal in photo- and hadro-production.

# 1 Introduction

A large volume of data now exists on the hadro-production of  $J/\psi$  at fixed target energies— both for the total cross section and the  $x_F$  distribution. In particular, several new experiments have taken high statistics data with pion or proton beams. Since a promising new model for heavy-quarkonium production is now available, it is useful to perform an analysis in the context of this model. This is the purpose of this paper.

The physics of heavy quarks can be expected to be dominated by its (large) mass,  $m$ , and hence computable in perturbative QCD. However, for quarkonium systems the scales  $mv$  (relative momentum) and  $mv^2$  (energy) are also important, since the quarks are expected to be non-relativistic in the rest frame of the quarkonium. An organised way to include the effects of the dimensionless parameter  $v$  (relative velocity) is provided by an effective low-energy field theory called non-relativistic QCD (NRQCD) [1].

A cutoff of the order of  $m$  is introduced [2] into the QCD action to remove all states of momenta larger than  $m$ . Their effects are taken into account through new couplings, which are local since the excluded states are relativistic. Beyond the leading order in  $1/m$  the effective theory is non-renormalisable. This cut-off theory is block-diagonalised to decouple the heavy-quark degrees of freedom, leaving a non-relativistic Schrödinger field theory. Consequently, states of a quark anti-quark pair can be specified by the spin, orbital and total angular momentum ( $^{2S+1}L_J$  in spectroscopic notation), a radial quantum number and the colour representation. Gluons emitted by quarks can be specified in a multipole expansion. The formalism of NRQCD has been successfully applied to first principles lattice computations of quarkonium spectra [3].

In this framework, a  $c\bar{c}$  pair is created by a short-distance process, and it binds into a quarkonium state over scales that are longer by powers of  $1/v$ . Assuming factorisation, the cross-section for the production of a meson  $H$  can be written as

$$\sigma(H) = \text{Im} \sum_{n=\{\alpha,S,L,J\}} \frac{F_n}{m^{d_n-4}} \langle \mathcal{O}_\alpha^H(^{2S+1}L_J) \rangle \quad (1)$$

where  $F_n$ 's are short distance matrix elements and  $\mathcal{O}_n$  are local 4-fermion operators, of naive dimension  $d_n$ , describing the long-distance physics (the angular brackets denote a vacuum expectation value). The cutoff-dependence

of  $F_n$  is compensated by that of the long-distance matrix elements. The colour index  $\alpha$  can run over singlet as well as octet representations.

The short-distance coefficients  $F_n$  have the usual perturbation expansion in powers of  $\alpha_s$ . The scaling of the matrix element  $\langle \mathcal{O}_\alpha^H(2S+1L_J) \rangle$  with  $v$  is determined by the (rotational) tensor representation of the gluonic transition connecting the state of the produced pair to the target hadron. Consequently, the sum in eq. (1) is a double power series expansion in  $v$  and  $\alpha_s$ . For bottomonium states,  $v^2$  is small compared to  $\alpha_s(m^2)$  and hence colour octet contributions are not very significant except when the singlet terms vanish. As a result, the expansion is close to the normal perturbative expansion. For charmonium states, a numerical coincidence,  $v^2 \sim \alpha_s(m^2)$ , makes the double expansion more complicated.

The importance of colour octet pieces were first seen [4] in the phenomenology of  $P$ -state charmonium production at large  $p_T$  in Tevatron data [5]. These processes do not have a consistent description in terms of colour singlet operators only [6]. However, even for the direct production of  $S$ -states such as the  $J/\psi$  or  $\psi'$ , where the colour singlet components give the leading contribution in  $v$ , the inclusion of sub-leading octet states was seen to be necessary for phenomenological reasons [7]. This can be understood in terms of the numerical coincidence of  $v$  and  $\alpha_s$  mentioned earlier.

Since the long-distance matrix elements are not calculable, and the octet matrix elements are not easily written in terms of decays, the Tevatron data must be used to fix these unknown parameters [8]. As a consequence, quantitative test of this formalism can come only from other experiments. Fixed-target experiments provide such tests, because colour-singlet contributions are expected to be negligible for photo-production and hadro-production of  $J/\psi$  in appropriate kinematic regions. A new linear combination of octet matrix elements appears here. In Ref. [9] this combination has been fixed through an analysis of elastic photo-production data.

In an earlier paper [10], we had considered data on hadro-production of  $J/\psi$  in proton-nucleon and pion-nucleon collisions at centre of mass energies,  $\sqrt{S}$ , upto about 60 GeV. We found that the data on forward ( $x_F > 0$ ) integrated cross sections are well described by the inclusion of octet components. These are parameter-free predictions, because the values of all the required non-perturbative matrix elements are derived from other experiments. In this paper, we carry out a more detailed investigation of the  $x_F$  and  $y$  distributions of  $J/\psi$  production for the same fixed-target energies. These are

given in Sections 2 and 3.

The octet model predictions for  $J/\psi$  production in fixed-target experiments have also been considered in Ref. [11, 12]. In Ref. [12] it is claimed that the ratio of directly produced  $J/\psi$  to  $\chi$  states is not in agreement with data. This is disputed in Ref. [11]. We address this question in Section 4. Our results are in agreement with those of Ref. [11].

## 2 Cross Sections

The  $x_F$  distribution for inclusive production of  $J/\psi$  can be written as a sum over all possible channels in the form

$$\frac{d\sigma_{J/\psi}}{dx_F} = \sum_{n=\{\alpha,S,L,J,H\}} \frac{d\sigma^n}{dx_F} \langle \mathcal{O}_\alpha^H(2S+1L_J) \rangle BR(H \rightarrow J/\psi). \quad (2)$$

A channel is specified by the rotational and colour quantum numbers of the  $c\bar{c}$  state, and the colour singlet meson it goes into. For both colour singlet and octet channels, the strong interaction effects required to bind a pair into a physical meson are specified by the matrix element  $\langle \mathcal{O} \rangle$ . Subsequently, this meson decays into the  $J/\psi$  with a branching ratio specified by  $BR$ . The formulæ for the channel cross sections [13], matrix elements and branching ratios are collected in Table 1 for all the relevant channels.

The matrix element appearing in the octet  ${}^3S_1$  channel with the gluon initiated part of the reaction is the combination

$$\Theta = \langle \mathcal{O}_8^{J/\psi}({}^1S_0) \rangle + \frac{3}{m^2} \langle \mathcal{O}_8^{J/\psi}({}^3P_0) \rangle + \frac{4}{5m^2} \langle \mathcal{O}_8^{J/\psi}({}^3P_2) \rangle. \quad (3)$$

Precisely this combination appears in the cross section for photo-production of the  $J/\psi$ , and has been fitted to the relevant data [9]. The two matrix elements in the singlet  ${}^3P_J$  state are related to the derivative of the wavefunction of  $\chi_J$  at the origin by

$$\langle \mathcal{O}_1^{\chi_J}({}^3P_J) \rangle = \frac{9(2J+1)}{2\pi} |R'(0)|^2. \quad (4)$$

It has been fixed by decay rates [14]. Each of the three octet  ${}^3P_J$  matrix elements have been extracted from hadro-production rates at the Tevatron.

$H$	$\alpha$	$^{2S+1}L_J$	$\frac{d\sigma}{dx_F}$	$\langle \mathcal{O}_\alpha^H(^{2S+1}L_J) \rangle$	$BR$ (%)
$J/\psi$	8	$^1S_0, ^3P_0, ^3P_2$	$\mathcal{L}_g \frac{5\alpha_s^2 \pi^3}{48m^5}$	$0.020 \pm 0.001 \text{ GeV}^3$	100
$J/\psi$	8	$^3S_1$	$\mathcal{L}_q \frac{\alpha_s^2 \pi^3}{54m^5}$	$0.0066 \pm 0.0021 \text{ GeV}^3$	100
$\chi_0$	1	$^3P_0$	$\mathcal{L}_g \frac{\alpha_s^2 \pi^3}{48m^7}$	$0.32 \pm 0.04 \text{ GeV}^5$	$0.66 \pm 0.18$
$\chi_0$	8	$^3S_1$	$\mathcal{L}_q \frac{\alpha_s^2 \pi^3}{54m^5}$		$0.66 \pm 0.18$
$\chi_1$	8	$^3S_1$	$\mathcal{L}_q \frac{\alpha_s^2 \pi^3}{54m^5}$	$0.0098 \pm 0.0013 \text{ GeV}^3$	$27.3 \pm 1.6$
$\chi_2$	1	$^3P_2$	$\mathcal{L}_g \frac{\alpha_s^2 \pi^3}{180m^7}$	$0.32 \pm 0.04 \text{ GeV}^5$	$13.5 \pm 1.1$
$\chi_2$	8	$^3S_1$	$\mathcal{L}_q \frac{\alpha_s^2 \pi^3}{54m^5}$		$13.5 \pm 1.1$

Table 1: The cross sections, non-perturbative matrix elements and branching ratios into the  $J/\psi$  for each channel (specified by the colour representation  $\alpha$ , rotational quantum numbers and the primary meson  $H$ ) relevant to the inclusive  $J/\psi$  cross section of eq. (2). The gluon and quark luminosities are defined in eq. (6). The value of the matrix element quoted in the first line is for the linear combination of eq. (3).

We use the tabulation of [15], along with the relation

$$\langle \mathcal{O}_8^{\chi_J}({}^3S_1) \rangle = (2J + 1) \langle \mathcal{O}_8^{\chi_0}({}^3S_1) \rangle. \quad (5)$$

The value of this matrix element for  $J = 1$  is shown in Table 1.

The gluon and quark luminosities,  $\mathcal{L}_g$  and  $\mathcal{L}_q$  respectively, are defined in terms of the relevant parton distributions in the projectile (P) and target (T), through the formulæ—

$$\begin{aligned} \mathcal{L}_g &= \frac{1}{\sqrt{x_F^2 + 4\tau}} x_+ g_P(x_+) x_- g_T(x_-), \\ \mathcal{L}_q &= \frac{1}{\sqrt{x_F^2 + 4\tau}} \left[ \sum_f x_+ q_P^f(x_+) x_- \bar{q}_T^f(x_-) + (P \leftrightarrow T) \right], \end{aligned} \quad (6)$$

where the sum in the definition of  $\mathcal{L}_q$  is over flavours. We have used the notation

$$x_{\pm} = \frac{1}{2}(\sqrt{x_F^2 + 4\tau} \pm x_F). \quad (7)$$

We also discuss briefly existing data on rapidity ( $y$ ) distributions of the  $J/\psi$ . These can be easily obtained from the  $x_F$  distribution by multiplying the latter with the Jacobian factor  $\sqrt{x_F^2 + 4\tau}$  for the transformation between  $x_F$  and  $y$ . It is clear that the dependence of the cross sections on  $x_F$  or  $y$  comes entirely from these luminosities.

Before discussing our computations and the comparison with data, we would like to note that the colour octet model contains many parameters in the form of non-perturbative matrix elements. Our approach here is to fix these values from different experiments and use the fixed target hadro-production data as a test of the phenomenological viability of the model.

### 3 Results

Before embarking on the computation of cross sections there are the usual choices for QCD inputs to be fixed up. From open charm production, the limits on the charm quark mass are  $1.2 \text{ GeV} \leq m \leq 1.8 \text{ GeV}$  [16]. In an earlier calculation of the total forward cross section,  $\sigma(x_F > 0)$  [10], we had varied  $m$  between 1.6 GeV and 1.7 GeV to obtain an agreement between the

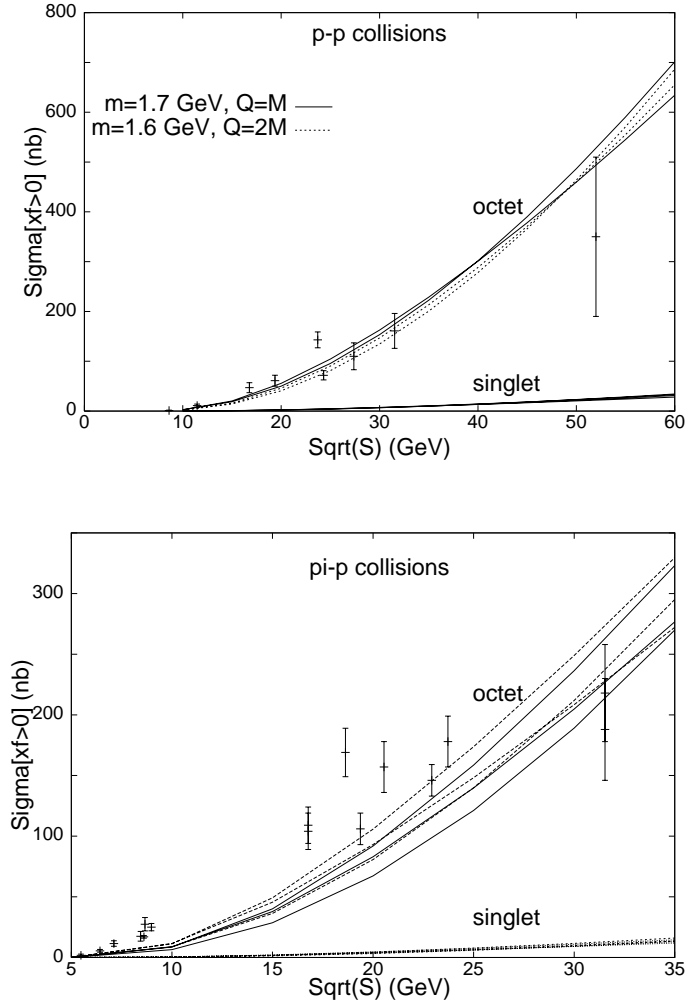


Figure 1: The colour-octet model predictions for integrated forward  $J/\psi$  hadroproduction cross sections as a function of the CM energy. For  $pp$  collisions, the two curves for each choice of  $m$  and scale  $Q$  are for the structure functions MRS D- $'$  and GRV LO. For  $\pi p$  collisions the three sets of structure functions are MRS D- $'$  for proton and SMRS 1 for  $\pi$ , MRS D- $'$  for proton and SMRS 3 for  $\pi$ , GRV LO for both. Note that the colour-singlet model predictions lie far below the data.

data and model computations. The QCD scale,  $Q$ , was varied between  $M$  and  $2M$  (where  $M$  is the mass of the  $J/\psi$ ). For these calculations we had used the MRS D-’ and the GRV LO sets of parton densities for the proton, and the SMRS 1, SMRS 3 and GRV densities for the pion. All the sets were taken from the PDFLIB package [17]. We continue with these choices here.

The total forward cross sections are shown in Figure 1. We would like to point out the following features—

- The colour singlet model predictions lie far below the data. The addition of the octet channels is necessary for the phenomenology.
- For  $pp$  collisions, all the data lie on the curves shown, with the exception of the data from [18]. The total forward cross section with a 300 GeV proton beam, reported in [18], is  $143 \pm 17$  nb. This is much higher than the corresponding number,  $71.8 \pm 9.3$ , reported by [19] from a 315 GeV proton beam. It would be useful to have a third experiment to sort out this mismatch.
- For  $\pi p$  collisions the data are very scattered. More data would be very welcome. The structure functions for  $\pi$  are also rather badly known, and this shows up as a bigger spread in the model prediction. Further experiments on high-mass lepton pair production with pion beams could reduce this uncertainty.
- The data at the highest energies (ISR) seem to prefer a smaller value of  $m$ . We discuss this point later.

In Figure 2, we compare the model with data on  $x_F$  distributions from three different  $pp$  experiments [18, 20, 21]. There is extremely good agreement for proton beam energy of 800 GeV over the 4 orders of magnitude spanned by the data [21]. Since the data sample contains  $2.45 \times 10^5$  events, the quoted errors are very small and the agreement is very significant. Data at other beam energies are also well described. The  $x_F$  distribution at 300 GeV energy [18] has been normalised by the ratio of their measured value of  $\sigma(x_F > 0)$  and the model prediction. There is no statistically significant evidence of a systematic deviation from the model predictions at large  $x_F$ . At large values of  $x_F$  the 300 GeV data may lie slightly below the model (but with statistically insignificant deviation). On the other hand, data in

the last  $x_F$  bin for the 800 GeV set lies a little above the prediction. Note also that only the statistical errors on the data are shown in the figures.

Figure 3, shows the  $x_F$  distributions in  $\pi-p$  collisions. The data are taken from three different experiments [18, 22, 23]. At the highest beam energy of 515 GeV, the data agrees extremely well with the model predictions both in magnitude and shape. At lower beam energies the shape is reproduced extremely well, although the agreement in magnitude is less perfect. It is not possible to decide whether this is due to nuclear effects or the pion structure functions, or even experimental uncertainties in the normalisation (see Figure 1). More data would help in deciding between these possibilities.

There is a small body of literature on cross sections and distributions in  $\bar{p}p$  collisions. The data on total forward cross sections is even more scattered than the pion data. Also, the number of  $J/\psi$  events are rather low, and hence lead to larger errors. For these reasons we have not attempted a quantitative study of this data.

Since a large amount of data exists for the differential cross section  $d\sigma/dy$  at  $y = 0$  in  $pp$  collisions, we have also tested the model against this. The data goes from values of  $\sqrt{S}$  near threshold upto ISR energies. The comparison of model and data are shown in Figure 4. It is clear that the data on the rapidity distribution is more scattered than that on total forward cross sections. In several cases experiments at the same value of  $\sqrt{S}$  yield values for the distribution which are not in agreement even when errors are taken into account. Nevertheless, a reasonable overall agreement of the model with the data can be seen.

It is interesting to note, however, that the low  $\sqrt{S}$  data prefer a larger value of the charm quark mass,  $m$ , and a smaller scale  $Q$  than the ISR data. As shown in the figure, this trend holds for both the total forward cross section and the rapidity distribution. A similiar observation used to be made for single inclusive charm production, before higher order perturbative calculations resolved this problem [24]. The essential physics is that higher orders are important near threshold because an off-shell heavy quark can be thrown on-shell by soft radiation. It seems reasonable to expect that similiar effects are at work here. Further study would call for inclusion of higher order perturbative effects.

Very naively one may have thought of tuning  $m$  and  $Q$  in order to produce the best results. However, since such a tuning would depend on  $\sqrt{S}$ , it is clearly not the correct way to proceed. In fact, as is now well-known, such

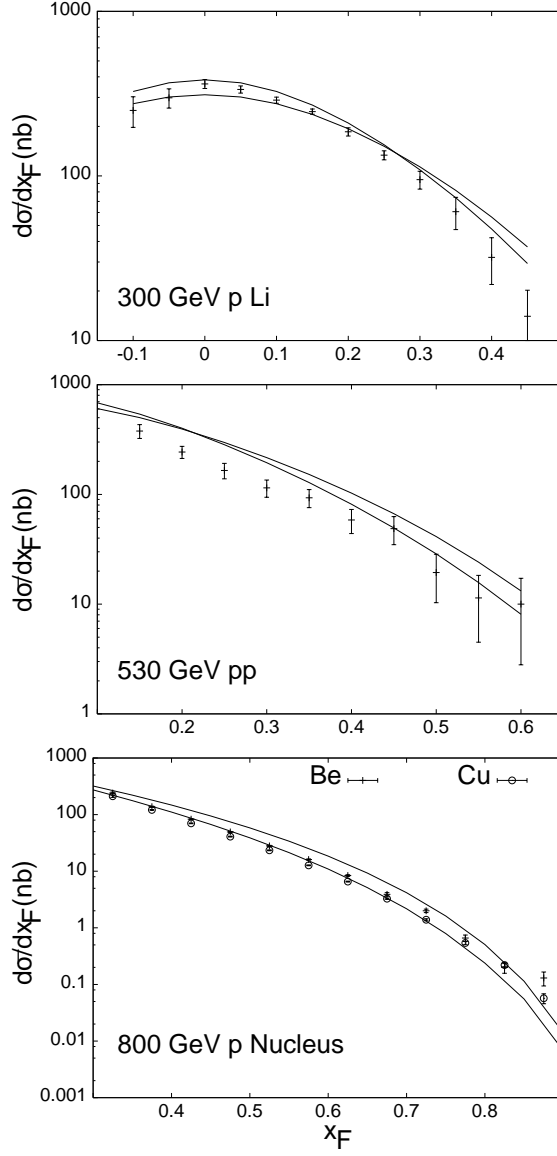


Figure 2: The colour-octet model predictions for the cross section differential in  $x_F$  for  $J/\psi$  production in  $pp$  collisions for different beam energies. The two curves are for the parton density sets MRS D-' and GRV LO and  $m = 1.7$  GeV and  $Q = M$ .

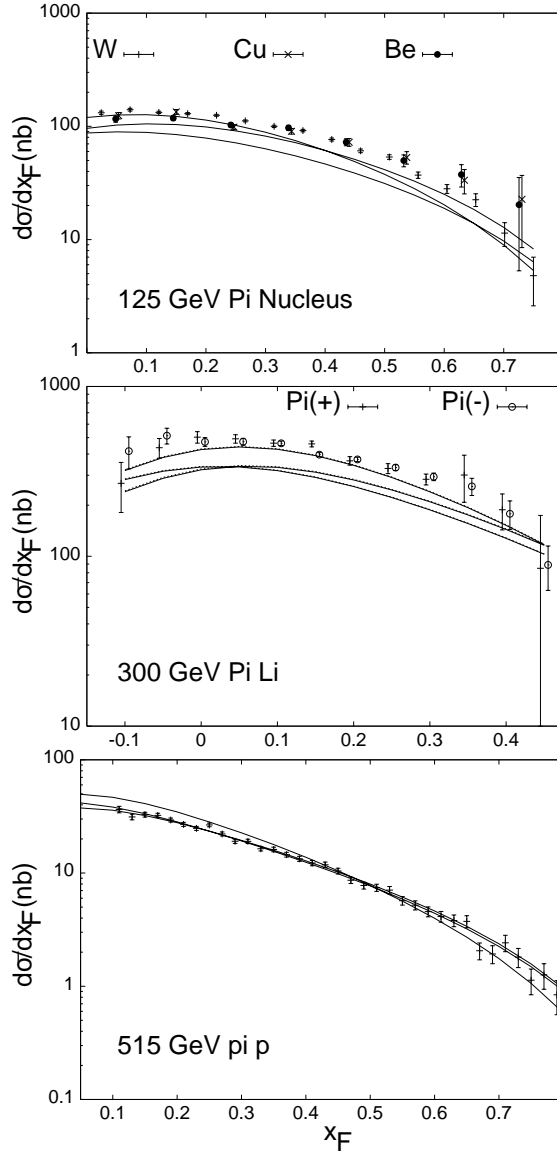


Figure 3: The colour-octet model predictions for the cross section differential in  $x_F$  for  $J/\psi$  production in  $\pi p$  collisions for different beam energies. The two curves are for the parton density sets MRS D- $'$  and GRV LO and  $m = 1.7$  GeV and  $Q = M$ . For visibility, the  $\pi^+$  and  $\pi^-$  data for beam energy 300 GeV have been offset equally to either side of the true  $x_F$  value. This is also done for the Cu and Be data at 125 GeV.

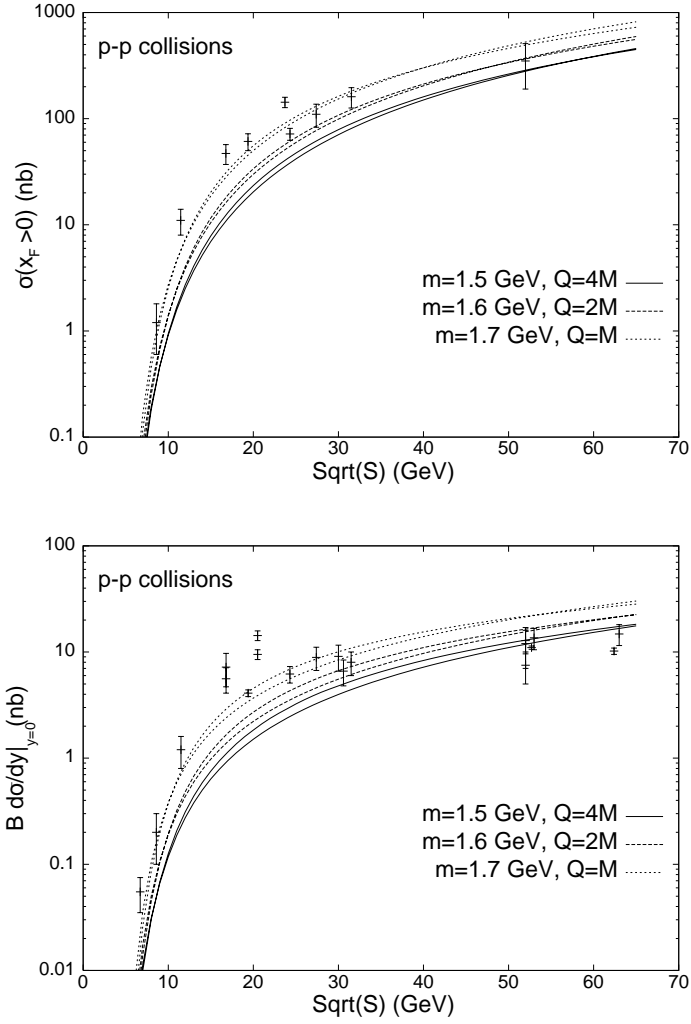


Figure 4:  $\sigma(x_F > 0)$  for  $J/\psi$  production in  $pp$  collisions (upper panel) and the differential cross section  $Bd\sigma/dy$  at  $y=0$  (lower panel), shown as a function of  $\sqrt{S}$ . For the model calculation we have assumed that the branching ratio for the decay of the  $J/\psi$  into leptons ( $B$ ) is 5.97%.

Source of uncertainty	$pp$	$\pi p$
Parton density sets	20%	29%
Scale uncertainties	91%	96%
Non-perturbative matrix elements	5%	5%

Table 2: Estimates of the magnitude of various theoretical uncertainties in the colour octet model for  $J/\psi$  production at  $\sqrt{S} = 19.4$  GeV. These are obtained from a calculation of  $d\sigma/dx_F$  at  $x_F = 0$ .

sensitive dependence on the scale is an artifact of leading order perturbative QCD calculations. Once higher orders are computed, it is possible to remove this strong dependence on  $Q$  and then fix the best values for  $m$  [16]. Hence, we may take the joint dependence of the cross sections on  $m$  and  $Q$  as an estimate of the importance of higher order perturbative QCD effects.

The magnitudes of the various theoretical uncertainties are summarised in Table 2. The errors on the individual non-perturbative matrix elements are quoted in Table 1. The dominant channel in eq. (2) is the gluon fusion part of the octet  $J/\psi$  (the other channels are suppressed either by a branching ratio or by  $\mathcal{L}_q/\mathcal{L}_g$ ). As a result, the corresponding matrix element dominates this source of uncertainty. The error quoted in the table above is a 1- $\sigma$  limit. Even if it is replaced by a 3- $\sigma$  limit, the uncertainty due to the matrix elements remains the smallest source of error. Scale uncertainties in the cross section are a factor of two. As discussed in the previous paragraph, these may be taken as a rough estimate of the importance of higher order perturbative QCD effects.

Apart from the model discussed in this paper, another, called the semi-local duality model (SLD) [25], is also used to describe charmonium cross sections. This model fixes cross sections for individual charmonium states by comparison with data on the total cross section at some value of  $\sqrt{S}$ . Once this is done, the results [26] for  $\sqrt{S}$  dependence and  $x_F$  are similar to those reported here. A distinction can perhaps be made with accurate data at large  $x_F$ , since SLD predicts a somewhat harder  $x_F$  distribution. Other

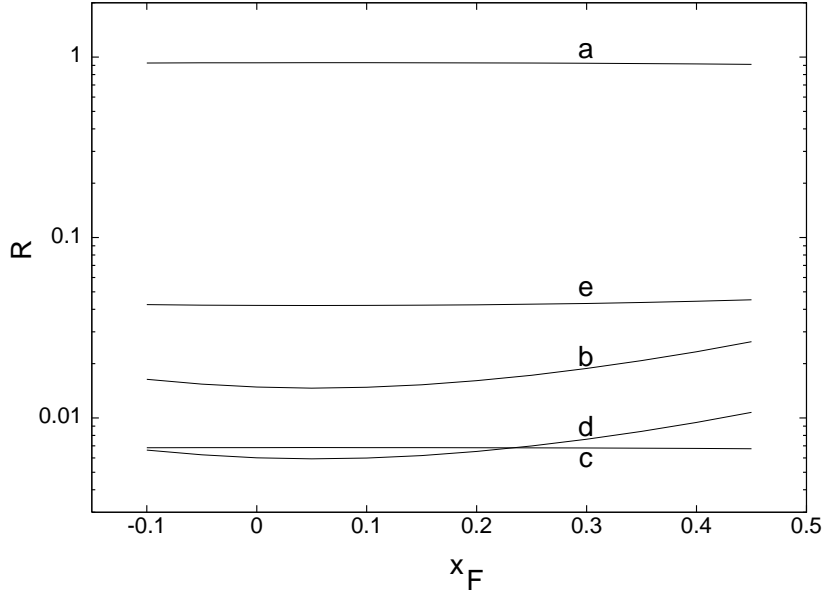


Figure 5:  $R$ , the fraction of  $d\sigma/dx_F$  as a function of  $x_F$  in to the channels (a)  $gg \rightarrow J/\psi$ , (b)  $qq \rightarrow J/\psi$ , (c)  $\chi_0$ , (d)  $\chi_1$  and (e)  $\chi_2$  production.

distinctions are possible [11], and will be discussed elsewhere.

## 4 Discussion

Next we turn to the ratio  $\sigma(\chi)/\sigma(J/\psi)$ . All the hard cross sections in Table 1 are taken to order  $\alpha_s$ . The non-perturbative matrix elements in the  $\chi_J$  channels are all of leading order in the velocity—  $v^2$ , and there are no contributions at order  $v^4$ . The octet terms for  $\chi_J$  are suppressed relative to the singlet terms by  $\mathcal{L}_q/\mathcal{L}_g$ . The contribution to direct  $J/\psi$  production starts at order  $v^4$ . Although sub-leading in  $v$ , it happens to be the channel with the largest contribution (see Figure 5) since it is gluon initiated and hence comes with a factor of  $\mathcal{L}_g$ . The  $\chi_1$  state, which has the largest branching fraction into  $J/\psi$  has no singlet contribution and hence is also by  $\mathcal{L}_q/\mathcal{L}_g$ .

From this discussion it is clear that the relative magnitudes of the parton luminosities,  $\mathcal{L}_g$  and  $\mathcal{L}_q$ , are important in determining the dominant production channels, and may offset the power counting in  $v$  to some extent. At

order  $v^6$  there are no new contributions to direct  $J/\psi$  production, but  $\chi_1$  is produced through gluon initial states. Therefore, we have to consider all production channels upto order  $v^6$  to get the  $\chi$  to direct  $J/\psi$  ratio. Beyond the order  $v^6$  terms, power counting in  $v$  can be used to truncate the NRQCD series at any desired level of accuracy, since all the dominant  $\mathcal{L}_g$  type terms are accounted for at order  $v^6$ .

Enumerating all possible processes at this order, we find that a certain linear combination,  $\Phi$ , of  $\langle \mathcal{O}_8^{\chi J}(^1S_0) \rangle$ ,  $\langle \mathcal{O}_8^{\chi J}(^3P_{0,2}) \rangle$  and  $\langle \mathcal{O}_8^{\chi J}(^3D_{J'}) \rangle$  is required for the hadro-production cross section [27]. These arise equally from quark and gluon initiated processes and hence the same linear combination  $\Phi$  is associated with both  $\mathcal{L}_g$  and  $\mathcal{L}_q$ . Analysis of the diagrams shows that precisely the same linear combination appears also in the photo-production cross section.

Two interesting consequences now emerge as predictions of the NRQCD approach to quarkonium production—

1. There are three families of matrix elements involved in  $\Phi$ . Each scales as  $(2J + 1)$  (with order  $v^2$  corrections) [2] where  $J$  is the spin of the  $\chi$  state. This gives—

$$\frac{\sigma(\chi_1)}{\sigma(\chi_2)} = \begin{cases} \frac{3}{5} & \text{(NRQCD),} \\ 0.62 \pm 0.18 \pm 0.09 & \text{(experiments).} \end{cases} \quad (8)$$

Within NRQCD, the predicted ratio does not depend on whether the mesons are photo- or hadro-produced. Nor does it depend on  $\sqrt{S}$ . The measurement quoted above comes from a global analysis of hadro-production experiments [28]. There are no studies of this ratio in photo-production. We would like to urge experimentalists to perform such a measurement.

2. In photo-production the ratio of  $\chi$  and direct  $J/\psi$  production is determined by the the ratio of the terms in  $\Phi$  and  $\Theta$  (eq. 3). As a result this ratio is independent of  $\sqrt{S}$ . In hadro-production this ratio is altered a little by the contribution of the colour-singlet production of  $\chi_0$  and  $\chi_2$ . The ratio increases by about 0.05 (see Figure 5). A small  $\sqrt{S}$  dependence is also to be expected in hadro-production due to the  $\sqrt{S}$  dependence of  $\mathcal{L}_q/\mathcal{L}_g$ . This may cause the ratio to be slightly

larger at small values of  $\sqrt{S}$ . A detailed numerical treatment will be presented elsewhere [27]. Data on this ratio from hadro-production yields the value  $0.43 \pm 0.04 \pm 0.04$  [28], almost independent of  $\sqrt{S}$ . In photo-production there is only the limit  $(\chi_1 + \chi_2)/(J/\psi) < 34\%$  (90% CL) [29]. Data on this ratio from photo-production experiments would constitute an important test of the NRQCD based colour-octet model.

The introduction of these order  $v^6$  terms does not change the inclusive  $J/\psi$  cross section because the value of  $\Theta$  extracted from photo-production has to decrease due to the inclusion of  $\Phi$ . The shape of the  $x_F$  distribution comes from the gluon luminosity. This is clear from Figure 5, since the ratio of the direct to total  $J/\psi$  differential cross section is constant. Since the order  $v^6$  contribution also comes from a gluon initiated process, and carries a factor  $\mathcal{L}_g$ , the shape of the  $x_F$  distribution remains unchanged. The net result of adding all contributions to the cross section upto order  $v^6$  is to change only the  $\chi$  to direct  $J/\psi$  ratio. A detailed study will be published later [27].

In summary, the colour-octet model based on NRQCD and an assumption about factorisation, written to order  $\alpha_s v^4$  gives a good phenomenological description of the total forward  $J/\psi$  cross section and the  $x_F$  and  $y$  distributions in hadroproduction at fixed target energies. A small discrepancy is found in extrapolating the fixed target results to ISR energies, but these are of a kind that have been earlier seen in single inclusive charm production and removed there by going to higher orders in  $\alpha_s$ . There is a discrepancy in the ratio of  $\chi$  to direct  $J/\psi$  production at order  $v^4$ . We have argued that this problem can be solved without changing the results on the cross section by extending the calculations to order  $\alpha_s v^6$ . Inclusion of these order  $v^6$  terms leads to two predictions— that for the  $\chi_1/\chi_2$  ratio is borne out by data, and the other, the rough equality of the  $\chi/J/\psi$  ratio in photo- and hadro-production can easily be tested in experiments. We believe that NRQCD provides a phenomenologically viable model for quarkonium production. Control of the next orders in the expansions in  $v$  and  $\alpha_s$  are, however, necessary. This work is now in progress [27].

## References

- [1] W.E. Caswell and G.P. Lepage, *Phys. Lett.*, B 167 (1986) 437.

- [2] G. T. Bodwin, E. Braaten and G. P. Lepage, *Phys. Rev.*, D 51 (1995) 1125.
- [3] P. Lepage *et al.*, *Phys. Rev.*, D 46 (1992) 4052;  
C. T. H. Davies *et al.*, *Phys. Rev.*, D 52 (1995) 6519;  
C. T. H. Davies *et al.*, *Phys. Rev.*, D 50 (1994) 6963;  
C. T. H. Davies *et al.*, *Phys. Lett.*, B 345 (1995) 42;  
C. T. H. Davies *et al.*, *Phys. Rev. Lett.*, 73 (1994) 2654.
- [4] E. Braaten, M. A. Doncheski, S. Fleming and M. Mangano, *Phys. Lett.*, B 333 (1994) 548;  
D. P. Roy and K. Sridhar, *Phys. Lett.*, B 339 (1994) 141;  
M. Cacciari and M. Greco, *Phys. Rev. Lett.*, 73 (1994) 1586.
- [5] F. Abe *et al.*, *Phys. Rev. Lett.*, 69 (1992) 3704 and *Phys. Rev. Lett.*, 71 (1993) 2537;  
K. Byrum, CDF Collaboration, Proceedings of the 27th International Conference on High Energy Physics, Glasgow, (1994), eds. P. J. Bussey and I.G. Knowles (Inst. of Physics Publ.) p.989.
- [6] G. T. Bodwin, E. Braaten and G. P. Lepage, *Phys. Rev.*, D 46 (1992) R1914.
- [7] E. Braaten and S. Fleming, *Phys. Rev. Lett.*, 74 (1995) 3327.
- [8] P. Cho and A. K. Leibovich, *Phys. Rev.*, D 53 (1996) 150.
- [9] N. Cacciari and M. Krämer, *Phys. Rev. Lett.*, 76 (1996) 4128;  
J. Amundson, S. Fleming and I. Maksymyk, UTTG-10-95, hep-ph/9601298.
- [10] S. Gupta and K. Sridhar, TIFR-TH-96-04, hep-ph/9601349, to appear in *Phys. Rev.*, D.
- [11] M. Beneke and I. Rothstein, *Phys. Rev.*, D 54 (1996) 2005.
- [12] W.-K. Tang and M. Vanttinen, NORDITA-96/18 P, hep-ph/9603266.
- [13] S. Fleming and I. Maksymyk, MADPH-95-922, hep-ph/9512320.
- [14] M. Mangano and A. Petrelli, *Phys. Lett.*, B 352 (1995) 445.

- [15] P. Cho and A. K. Leibovich, *Phys. Rev.*, D 53 (1996) 6203.
- [16] P. Nason, S. Frixione and G. Ridolfi, Invited talk at the International Conf. on Physics in Collisions, Cracow, Poland, Jun. 1995 (hep-ph/9510253).
- [17] H. Plochow-Besch, *Comp. Phys. Comm.*, 75 (1993) 396.
- [18] L. Antoniazzi *et al.*, *Phys. Rev.*, D 46 (1992) 4828.
- [19] C. Morel *et al.*, *Phys. Lett.*, B 252 (1990) 505.
- [20] V. Abramov *et al.*, Fermilab Preprint FERMILAB-PUB-91/62-E.
- [21] M. S. Kowitt *et al.*, *Phys. Rev. Lett.*, 72 (1994) 1318.
- [22] C. Akerlof *et al.*, *Phys. Rev.*, D 48 (1993) 5067.
- [23] A. Gribushin *et al.*, *Phys. Rev.*, D 53 (1996) 4723.
- [24] P. Nason, S. Dawson and R. K. Ellis, *Nucl. Phys.*, B 303 (1988) 607.
- [25] H. Fritzsche, *Phys. Lett.*, B 67 (1977) 217. F. Halzen, *Phys. Lett.*, B 69 (1977) 105.
- [26] R. Gavai *et al.*, *Int. J. Mod. Phys.*, A 10 (1995) 3043;  
J. Amundson *et al.*, preprint MADPH-96-942, hep-ph/9605295.
- [27] S. Gupta and K. Sridhar, work in progress.
- [28] V. Koreshev *et al.*, Fermilab Preprint, FERMILAB-PUB-96/093-E.
- [29] R. Barate *et al.*, *Z. Phys.*, C 33 (1987) 505.